



# A Thin and Low-Cost Scalable Waveguide Load Absorber

F. Nazari<sup>a</sup>, F. Ghorbani<sup>a</sup>, M.A. Khak<sup>a</sup>, P. J. Soh<sup>b,c</sup>, H. Aliakbarian<sup>a\*</sup>

<sup>a</sup>*Faculty of Electrical Engineering, K. N. Toosi University of Technology, Tehran, Iran,*

<sup>b</sup>*Advanced Communication Engineering (ACE) CoE, Faculty of Electronic Engineering Technology, Universiti Malaysia Perlis, Pauh Putra Campus, Perlis, Malaysia.*

<sup>c</sup>*Centre for Wireless Communication (CWC), University of Oulu, P.O. Box 4500, 90014 University of Oulu, Finland.*

---

## Abstract

In this paper, a set of simple S-band waveguide absorbers are designed and implemented on a low-cost FR4 substrate. This is to provide an alternative for conventional waveguide absorbers, which are generally bulky and costly. The proposed structure is composed of only two open-ended resonator strips on a low-cost, 3.2-mm thick FR4 board. These absorbers operate with the same fundamentals as absorbers based on the frequency selective surfaces. The proposed innovative waveguide absorber load is mode-independent and designed without any connection between the strips and the waveguide. Simulations and measurements indicated an approximately 2.2 % of bandwidth, with a 99 % absorption rate at the center frequency. A complete parameter study is also performed to show the robustness of the design, besides enabling tuning for use in other microwave waveguides. A good agreement between simulated and measured results confirms the functionality of the absorber.

**Keywords:** Waveguide absorber; Frequency Selective Surface, Waveguide load.

---

## 1. Introduction

Waveguide absorbers are widely used as a terminator in microwave networks. The unused ports in multiport networks should be terminated to avoid the open or shorted ports from affecting the performance of the overall system. Circulators, directional couplers, and magic-tees are such devices that need to be terminated with care. Termination of the unconnected port of hybrid dividers typically results in the improvements of reflection coefficients. Besides that, placement of an absorber in one of the circulator's port enables them to function as good isolators [1, 2].

---

\* Corresponding author. Tel.: +0-000-000-0000 ; fax: +0-000-000-0000 .  
E-mail address: [h.aliakbarian@ieee.org](mailto:h.aliakbarian@ieee.org).

Electromagnetic absorbers, in general, can be either classified according to their bandwidth, material, or structure type. Absorber types can be classified into three groups based on their bandwidths: narrowband, wideband, and ultra-wideband. Besides that, four classes of absorbers exist based on their materials: conductive absorber, dielectric absorber, magnetic absorber, and metamaterials. On the other hand, absorbers can also be classified from a structural point of view. In such cases, their categories include flat plate absorbers, quarter-wavelength absorbers, multi-layered absorbers, Jaumann absorbers [3], Chevron-shaped wave absorbers [4], and pyramidal wave absorbers [5].

Microwave waveguide absorbers usually capture incident waves using an absorbent material which is matched to the transmission medium. Ideally, when the incident wave hits the absorbing section, it observes no impedance discontinuity, and therefore, all of its energy is transferred into an absorbing medium where it is gradually dissipated and converted into heat [6]. The amount of absorption depends on factors such as its material properties, thickness, incident angle, etc. [7]. Conventional waveguide absorbers are widely used in microwave and millimeter-wave frequencies [1, 8-12]. They are broadband and usually contain single- or multi-layered structure of thick and bulky lossy materials. One of the topics of interest in waveguide absorbers is to minimize their size [12]. As shown in [12, 13], smaller absorber sizes can be realized using tapered structures made using graphite or ferrite, as is widely used in waveguide terminations. However, these structures are electrically large and limits their applications in compact devices. A potential solution to this includes the pyramidal polymer absorbers and metallic short circuit terminations, which can be implemented using 3D printing technology [1]. Such waveguide absorbers require a large volume and need a large waveguide area to be effective.

The thin plate of metamaterial absorber is analyzed as Frequency Selective Surfaces (FSS). Each unit cell in an FSS has a resonant frequency in which the electromagnetic energy is trapped and dissipated. There have been many designs of FSS absorbers considering their bandwidth, polarization, and their angular behavior. In previous works, the periodic structure of the FSS is used to absorb the radiated power in open space [14-20]. However, our aim is to design a small and thin waveguide absorber which is installed at the end of a waveguide. There are different configurations of the waveguide terminations. The waveguide absorber with two circular ring resonators is a common configuration that has been employed for X-band waveguide [21-23]. In [24] a waveguide absorber based on H-shaped resonator is presented at 10.5 GHz. Two other types of waveguide absorbers based on square-shaped and triangle-shaped resonators are investigated in [25]. In [26] a polarization-angle-independent fishnet-based waveguide absorber comprised of octagon shaped resonators is analyzed. The configurations presented in [22, 24, 26] need multi-layer PCB that makes them more expensive and complicated to realize. Moreover, in the mentioned works, the power handling haven't been analyzed.

The waveguide absorbers are located in a waveguide with good metallic boundary conditions, which can be modeled by image theory as a periodic structure without a waveguide. By using this concept, for the first time, we treat the proposed printed absorber as FSS. The simulation and measured results show the presented analysis can efficiently predict the performance of such absorbers. The high absorption rate and low production costs compared to other absorbers makes this type of waveguide absorber attractive [16, 24, 27].

In this paper, a very simple but innovative narrowband FSS waveguide absorber is introduced. The proposed architecture is composed of a pair of metallic stubs printed on a dielectric substrate. The absorption effectiveness of this low-cost, thin, and easily scalable solution is demonstrated inside an S-band waveguide. In contrast with a regularly printed absorber, the proposed absorber could be simply inserted in a waveguide without requiring any further soldering procedure.

In section II of this paper, the structure of the absorber is discussed. Power handling and the effect of incident angle are two important topics that are explained in detail in this section. The effects of the geometric parameter of the absorber are presented in part III of the main body of the article. In section IV, the

fabrication procedure and the measurement results are presented, and finally, the paper is concluded in section V.

## 2. Proposed Absorber Structure

The absorptivity of an absorber can be expressed as [6]:

$$A(\omega) = 1 - \Gamma(\omega) - T(\omega) = 1 - |S_{11}|^2 - |S_{21}|^2 \quad (1)$$

where  $\Gamma(\omega)$  and  $T(\omega)$  are the reflection and transmission coefficients, respectively, and can be calculated from the S-parameters,  $S_{11}$ , and  $S_{21}$ . To realize a completely absorptive structure, the reflection and transmission must be zero and  $A(\omega) = 1$  [28]. In a waveguide absorber, the end of the absorber is shorted. This then zeroes the transmission coefficient, enabling further efforts to be focused on minimizing the reflection coefficient. This is done by matching its impedance to free space. To study the effective impedance of the structure, the unit cell boundary condition is used in full-wave simulation.

The designed absorber in this work is aimed at decoupling the internal coupling between two slots in a waveguide slot array antenna while simultaneously keeping the external coupling unchanged. Such applications require a very narrow load which does not affect the field distribution on the slots but still absorbs most of the inserted power. The slot antenna and the absorber placed in the middle is presented in Fig. 1.

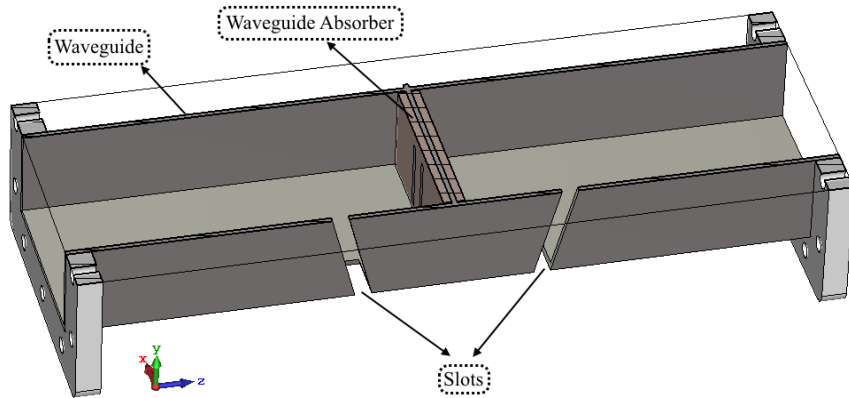


Fig. 1. Application of the waveguide absorber in eliminating internal coupling between two slots

Beside the free space matching goal, the defined structure should be as simple, low cost, and thin. At the same time, the absorber should be scalable to fit into any waveguide. Therefore, a single layer PCB is chosen to design the resonator, which is aimed at absorbing resonance at the target frequency. One of the simplest of such resonators is by designing two symmetrical parallel strips printed on one side of an FR4 substrate ( $\epsilon_r=4.3$ ,  $\tan\delta \approx 0.025$ ), and a ground plane on its reverse side, as shown in Fig. 2. It is designed as an absorber in the S-band WR-284 standard waveguide.

### 2.1. Resonance Analysis

The two resonant parallel strips are designed on the FR4 substrate with lengths of approximately less than  $\lambda_g/2$ . Parameter  $\lambda_g$  is accurately determined from the effective  $\epsilon_r$  [29].

Based on the thickness of the FR4 substrate and line width of 3.2 mm and 2.6 mm, respectively, the calculated  $\epsilon_{\text{reff}}$  is 3.13. This indicates a resonant strip length of  $0.44\lambda$  at 2.8 GHz. The incident waves resonant at this frequency will then be absorbed into the lossy substrate, provided that the strips is placed in the same direction as the electric field of the incident wave (the  $\text{TE}_{10}$  mode).

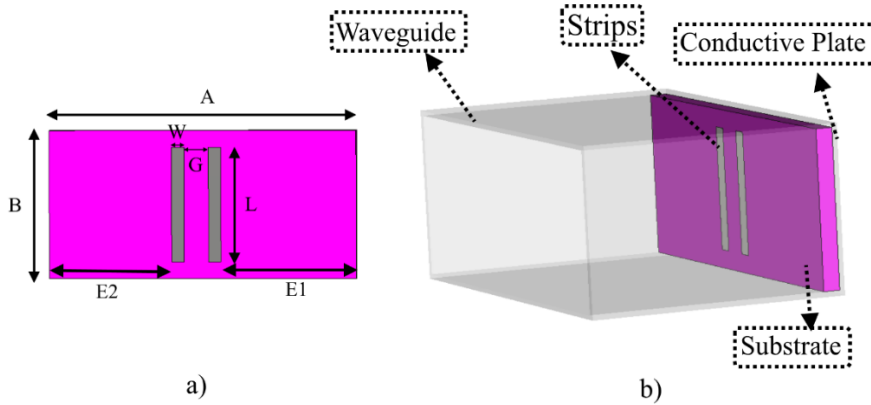


Fig. 2. Structure of the proposed absorber

Table 1 Main dimensional parameters of the structure

Parameters	Value(mm)
$A$	72.136
$B$	34.036
$L$	26.23
$W$	2.6
$G$	5.65
$E1$	31.3
$E2$	28.42
Substrate thickness	3.2

The proposed structure is modeled in CST Microwave studio by exciting a waveguide port and observing its reflection coefficient. The main dimensions of the proposed structure are summarized in Table 1, with the values of  $A$ ,  $B$  chosen based on the WR-284 dimensions. However, changes in these two parameters are insignificant on the performance of the absorber, and therefore indicating its mode independence. This also implies that the angle of the incident on the structure will not significantly affect its absorption performance.

## 2.2. Unit-Cell Analysis

Considering the electrical wall defined around the absorber in the waveguide and the image theory, simulations with unit cell boundary conditions can provide a good estimate of the EM properties of the

structure. The reflection, transmission, and absorption characteristics of the proposed structure with unit cell boundary conditions are presented in Fig. 3. In absorbers, reflections can be minimized by manipulating the effective permittivity and effective permeability. These two properties can be made equal at a target frequency by ensuring that the effective impedance of the FSS,  $Z(\omega) = \sqrt{\mu(\omega)/\varepsilon(\omega)}$  will match to free space and minimize reflections [25, 30].

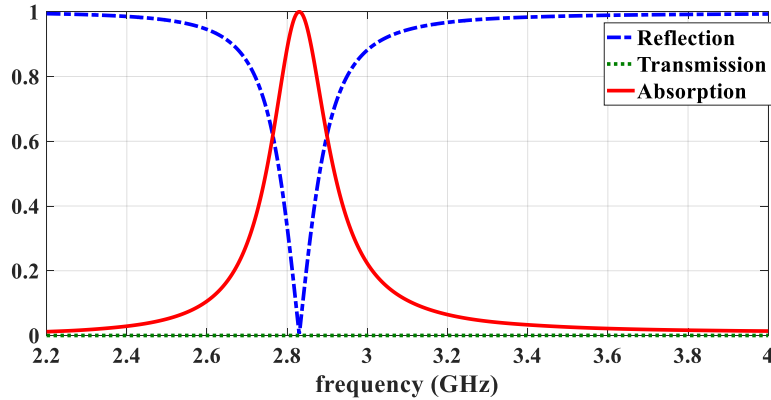


Fig. 3. Simulated reflection, transmission and absorption of the proposed absorber.

### 2.3. Power handling

The power handling of the proposed absorber highly depends on the substrate material and the substrate thickness. The maximum electric strength and maximum tolerable temperature are the main parameters that determine the maximum peak power and average power handling. While the maximum electric strength of FR4 substrates differs, the substrate datasheet in this work indicates this is approximately 39 KV/mm. In this structure, the closest distance between two metals (strip to ground distance of 3.2 mm) is the location where the peak electric field occurs. Simulations indicate that a 125 kW input power induces 124.8 KV between strips and the ground metallization, resulting in a 39 KV/mm of electric field. Assuming a margin of 50 %, a peak power of 60 KW is able to be handled by this absorber.

The maximum temperature able to be handled by the FR4 substrate is 135 °C (408 °K). However, the average power handling is dependent on the heat conduction from the absorber to heat sinks and to the external environment. Calculations indicate that the maximum peak power of around 3.6 KW generates such temperature in the substrate within one second. Without any thermal conductions, a 60 W input power for 60 s is capable of increasing the temperature of the absorber up to this critical value. Thus, higher average power can be tolerated by the absorber using a good cooling system.

### 2.4. Effect of incident angle

The angular performance is one of the main characteristics of microwave absorbers in general. The absorption rate is calculated based on the following:

$$\theta_i = \arcsin(f_c / f) = \arcsin(\beta / k), \quad f_c = C / 2A \quad (2)$$

where  $f_c$  is the cut-off frequency of the waveguide, which changes with the width of the waveguide ( $A$ ). The working frequency is represented by  $f$ , and  $k$  is the propagation constant in the medium (free space).

It is observed from Fig. 4 that the absorber works in the target 2.8 GHz for the incident angles of 30°, 45°, 60°, and 90°, which is equivalent to different waveguide sizes,  $\beta$ . This characteristic is especially important to ensure that the operation of the absorber strips are independent of their distance from the waveguide's walls. Nonetheless, a minor shift is existent between the results obtained from the normal incident angle (TEM incident) and the rest of the incident angles.

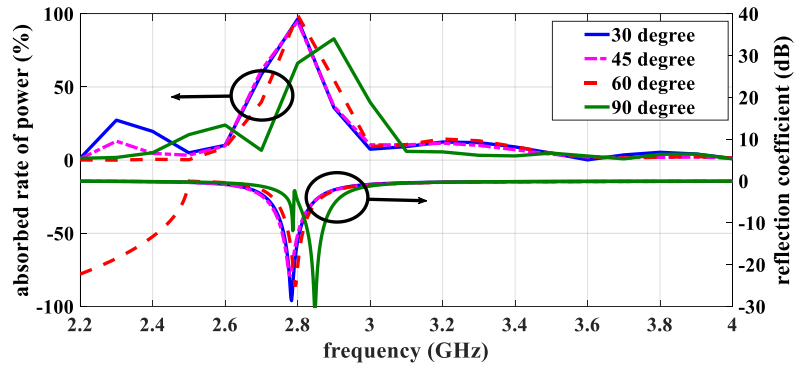


Fig. 4. Absorption rates and reflection coefficients of the proposed structure at different incident angles

### 3. Parameter Analysis

The thickness of the substrate directly affects the amount of absorbed power. As expected, simulation results show that the thicker the substrate, the higher the absorption rate. This is validated in Fig. 5 by changing the substrate thickness from 0.5 mm to 3 mm. The results also show that as this thickness is increased, there is a slight shift of the operating band towards the lower frequencies due to the change in the effective dielectric constant of the strip.

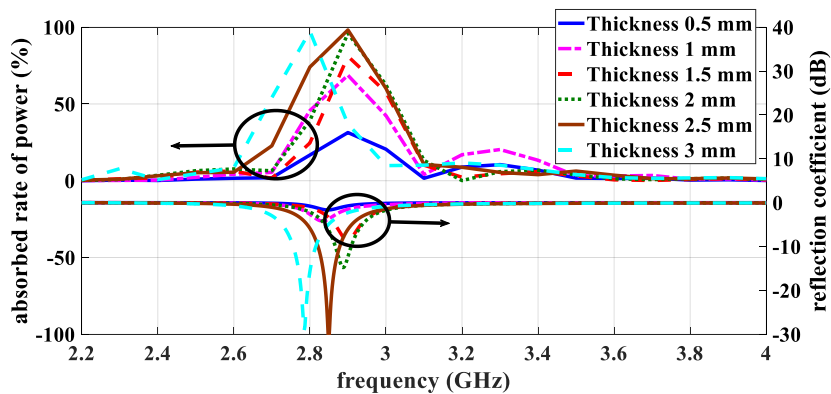


Fig. 5. Absorption rates and reflection coefficients of the proposed structure for different substrate thicknesses

However, it is found that the distance between the two strips is insignificant to the resonance of the absorbers, as shown in Fig. 6. Increasing the spacing between two strips from 3 mm to 6 mm decreases the

coupling and slightly increases the effective length, resulting in a slight decrease in resonance. However, a further increase in  $G$  increases resonance. This is caused by the movement of the strips away from the center of the waveguide. If this distance is more than 40 mm, the absorption rate decreases as the E-field level becomes negligible, as shown in Fig. 7. The current density on the strips for the two different values of  $G$  is higher when the two strips are located closer to each other and vice versa. For  $G = 10$  mm, the peak value of the current density is 166 A/m, whereas for  $G = 60$  mm, its value is 54 A/m.

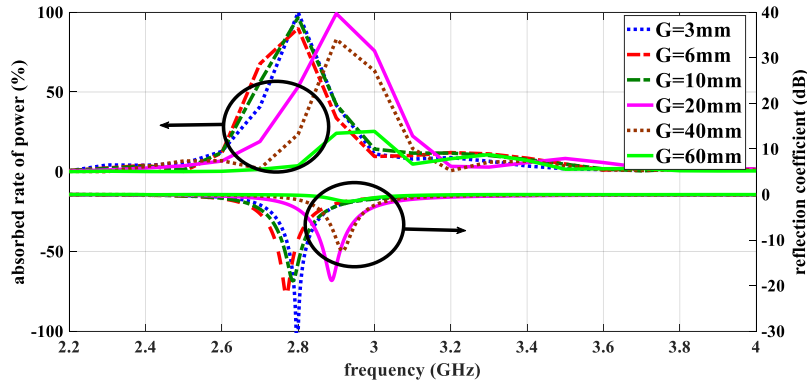


Fig. 6. Absorption rates and reflection coefficients of the proposed structure for different values of  $G$

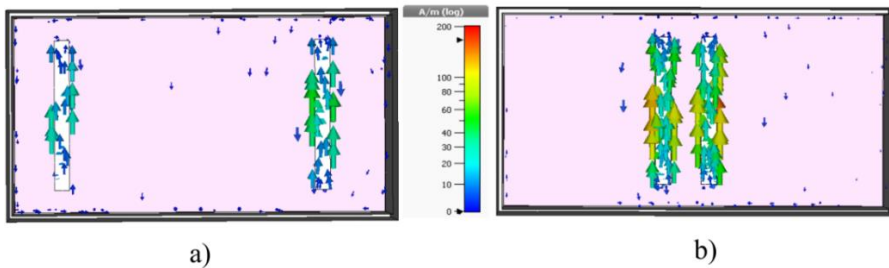


Fig. 7. Current density of the proposed structure for two different values of  $G$  a)  $G=60$  mm b)  $G=10$  mm

In the proposed structure, the value of  $L$  determines the resonant frequency of the strips and thus determines the operating frequency of the absorber. The absorption rate and reflection coefficient for different values of  $L$  illustrated in Fig. 8 indicated the adaptability of this concept to different frequencies. As the value of  $L$  increases from 18 mm to 30 mm, the bandwidth of the absorber decreases from 74 MHz to 45 MHz, while maintaining a consistent 1.8 % fractional bandwidth.

This concept has been used to design the set of waveguide absorbers for this application. The simplicity of the structure makes it a suitable design for low cost, low power, and narrowband applications. It is easily adaptable to other waveguides operating at different frequencies, and even several sheets of them can be replaced and used in the same waveguide. To demonstrate this, the designed absorber is scaled to other standard waveguides such as WR-187, WR-284, and WR-430. The dimensions of the absorbers for these different waveguides are summarized in Table 2. As shown in Fig. 9, the maximum power absorption rate of the three waveguides are located at 1.9 GHz, 2.8 GHz, and 4.7 GHz.

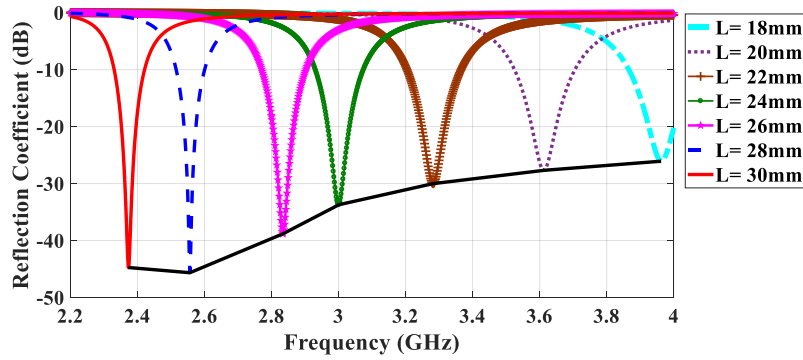


Fig. 8. Reflection coefficients and absorption rates of the proposed absorber for different values of  $L$

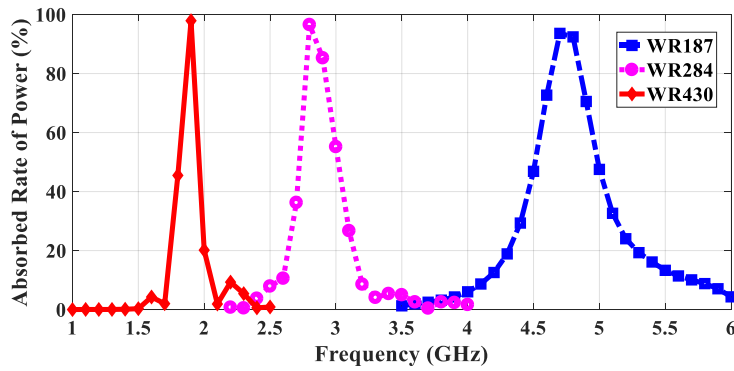


Fig. 9. Power absorption rate of the absorber in different waveguides.

Table 2 Dimension of the absorber in different waveguides

Parameters	WR-187	WR-284	WR-430
$A$ (mm)	47.55	72.136	109.22
$B$ (mm)	22.15	34.036	54.61
$L$ (mm)	15	26	40
$W$ (mm)	1.3	2.87	3.8
$G$ (mm)	2	5.65	7.3

#### 4. Fabrication and Measurement

The waveguide absorber is placed at the end of a WR-284 standard waveguide, as shown in Fig. 10, whereas a conductive plate is mounted on it after placing the absorber at the end of the waveguide. As aforementioned, tuning the proposed absorber to operate in different frequencies requires only the



modification of the length of the strips. As shown in Fig. 11, the three different lengths of 18 mm, 22mm, and 26 mm are employed to tune the resonant frequency of the absorber.

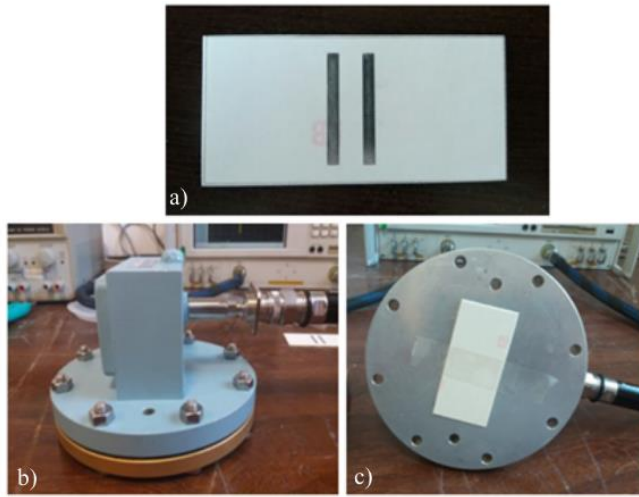


Fig. 10. a) Fabricated waveguide absorber, b) coaxial to waveguide transformer and the end plate c) the absorber prototype placed in the WR-284 waveguide

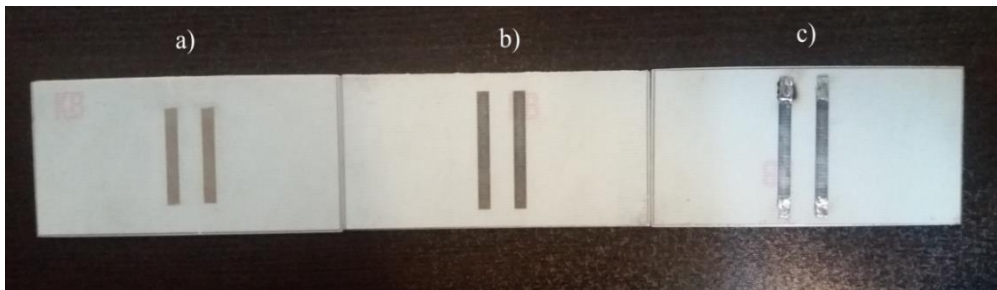


Fig. 11. Three absorbers with different strip lengths for resonance at three different frequencies a)  $L=18$  (at 3.96 GHz) b)  $L=22$  (at 3.27 GHz), c)  $L=26$  (at 2.83 GHz).

The simulated and measured reflection coefficients of all three fabricated waveguide absorbers are compared in Figs. 12-14. Only less than 3 % of the power is reflected back to the source, 4 % of the power is dissipated on the metals, the rest of the power, approximately 93 %, is absorbed in the dielectric. By defining the 10 dB frequency band of the reflection coefficient as the absorber's bandwidth, the simulated and measured bandwidth of the proposed structure with  $L = 26$  mm are 64 MHz and 58 MHz, respectively. This shows the good agreement of simulation and measurement.

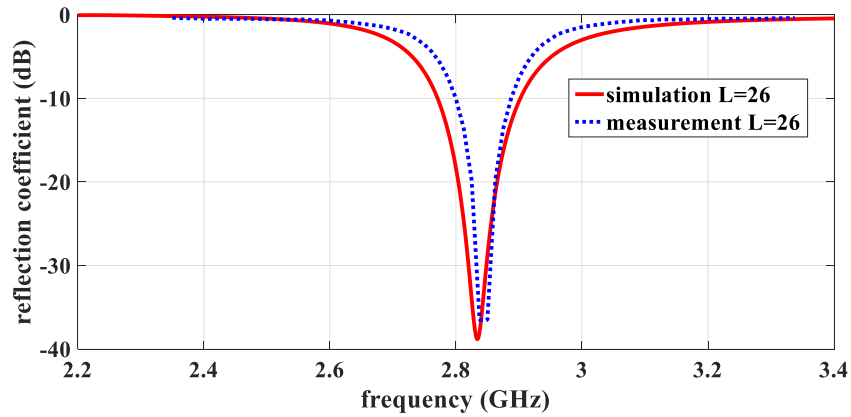


Fig. 12. Comparison between simulated and measured reflection coefficients of the waveguide absorber for different  $L=26$ .

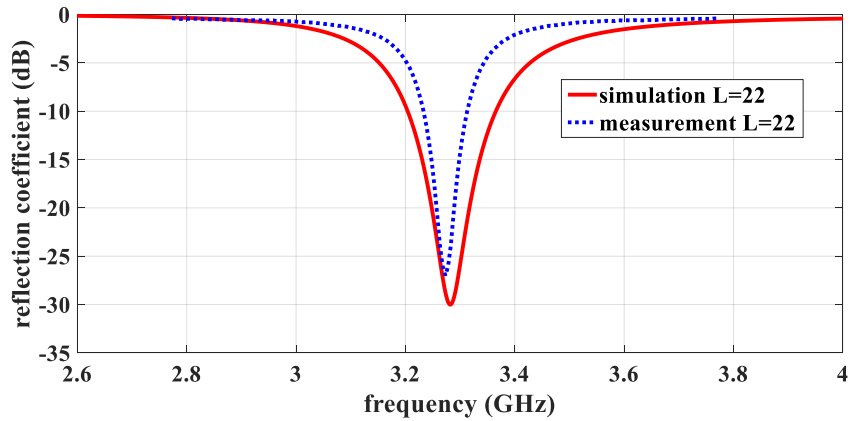


Fig. 13. Comparison between simulated and measured reflection coefficients of the waveguide absorber for different  $L=22$ .

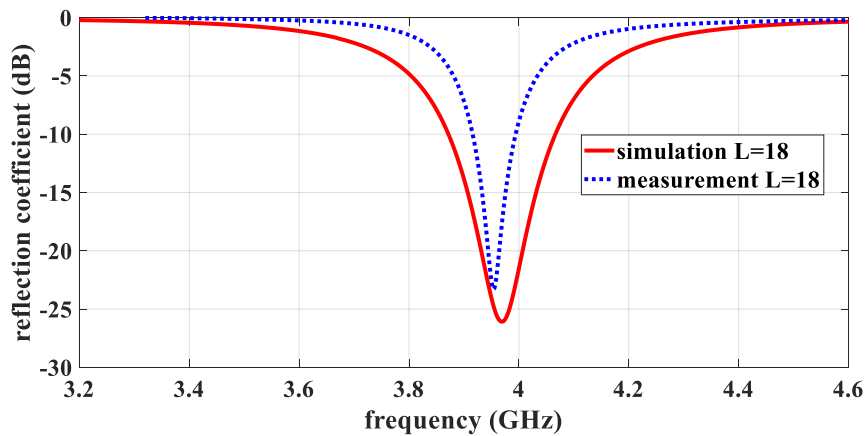


Fig. 14. Comparison between simulated and measured reflection coefficients of the waveguide absorber for different  $L=18$ .

The main characteristics of the proposed absorber against conventional pyramidal absorber and two other printed absorbers are summarized in Table 3. The proposed waveguide absorber is seen to be able to replace conventional waveguide absorbers, provided that the application is narrowband and relatively low power. This comparison also indicates that other more complicated structures such as [24], [30], and [25] are not necessarily better than the proposed simple, two-strip structure.

Table 3 Comparison of the proposed structure with different waveguide absorbers available in literature

Criteria	Proposed structure	[1]	[24]	[25]	[22]	[26]
<b>Structure</b>	Printed (2.5D)	Pyramidal (3D)	Printed (2.5D)	Printed (2.5D)	Printed (2.5D)	Printed (2.5 D)
<b>Thickness (Length)</b>	3.2 mm (0.03 $\lambda$ )	69.21 mm (2,3 $\lambda$ )	2 mm (0.067 $\lambda$ )	0.8 mm (0.03 $\lambda$ )	1.5 mm (0.05 $\lambda$ )	NA
<b>Cost</b>	Low (1layer PCB)	High	Medium (2layer PCB)	Low (1layer PCB)	Low (1layer PCB)	Medium (2layer PCB)
<b>Mode dependency</b>	No	No	No	No	NA	NA
<b>Reflection coefficient</b>	-37 dB	NA	-11 dB	-30 dB	-20 dB	-23 dB

## 5. Conclusion

In this paper, a simple waveguide absorber consisting of two strips printed on a layer of FR4 substrate is presented. This simple and narrowband structure can achieve about 99 % absorption rate and within a 3dB bandwidth of 64 MHz centered at 2.8 GHz. Considering the discharge threshold, the power handling of the absorber is found to be more than 100 KW. This is limited by the heating tolerance of the substrate, but can be mitigated by introducing a cooling system. Moreover, simulations show that the performance of the absorber is independent of the incident angle within the operating frequency of the designed strip. The effects of different geometrical parameters are also investigated in detail. Three prototypes of the absorber are fabricated for application on a WR-284 waveguide. Simulation and measurement results are in good agreement with each other and validated the absorber's scalability for use in other waveguides and operating bands.

## References

- [1] Y. Arbaoui *et al.*, "Full 3-D printed microwave termination: A simple and low-cost solution," *IEEE Transactions on Microwave Theory and Techniques*, vol. 64, no. 1, pp. 271-278, 2015.
- [2] P. K. Verma and R. Kumar, "Realization of Wide Band Waveguide Terminations at Ku-Band," *International Journal of Advances in Microwave Technology*, vol. 3, pp. 176-179, 2018.
- [3] E. Knott and C. Lunden, "The two-sheet capacitive Jaumann absorber," *IEEE Transactions on Antennas and Propagation*, vol. 43, no. 11, pp. 1339-1343, 1995.
- [4] Y. Mo, J. Zhong, and Y.-S. Lin, "Tunable chevron-shaped infrared metamaterial," *Materials Letters*, vol. 263, p. 127291, 2020.
- [5] Y. Kotsuka, *Electromagnetic Wave Absorbers: Detailed Theories and Applications*. John Wiley & Sons, 2019.
- [6] T. T. Nguyen and S. Lim, "Bandwidth-enhanced and Wide-angle-of-incidence Metamaterial Absorber using a Hybrid Unit Cell," *Scientific reports*, vol. 7, no. 1, pp. 1-11, 2017.

- [7] W. Zuo, Y. Yang, X. He, C. Mao, and T. Liu, "An ultrawideband miniaturized metamaterial absorber in the ultrahigh-frequency range," *IEEE Antennas and Wireless Propagation Letters*, vol. 16, pp. 928-931, 2016.
- [8] G. T. Ruck, *Radar cross section handbook*. Plenum Publishing Corporation, 1970.
- [9] E. F. Knott, "Radar cross section fundamentals," in *Radar Cross Section Measurements*: Springer, 1993, pp. 1-26.
- [10] B. Zhu, Z. Wang, C. Huang, Y. Feng, J. Zhao, and T. Jiang, "Polarization insensitive metamaterial absorber with wide incident angle," *Progress In Electromagnetics Research*, vol. 101, pp. 231-239, 2010.
- [11] Y. Cheng, H. Yang, Z. Cheng, and B. Xiao, "A planar polarization-insensitive metamaterial absorber," *Photonics and Nanostructures-Fundamentals and Applications*, vol. 9, no. 1, pp. 8-14, 2011.
- [12] B. Beuerle, J. Champion, U. Shah, and J. Oberhammer, "Integrated micromachined waveguide absorbers at 220–325 GHz," in *2017 47th European Microwave Conference (EuMC)*, 2017, pp. 695-698: IEEE.
- [13] E. Wollack, D. Fixsen, A. Kogut, M. Limon, P. Mirel, and J. Singal, "Radiometric-waveguide calibrators," *IEEE Transactions on Instrumentation and Measurement*, vol. 56, no. 5, pp. 2073-2078, 2007.
- [14] H.-T. Chen, A. J. Taylor, and N. Yu, "A review of metasurfaces: physics and applications," *Reports on progress in physics*, vol. 79, no. 7, p. 076401, 2016.
- [15] N. Engheta, "Thin absorbing screens using metamaterial surfaces," in *IEEE Antennas and Propagation Society International Symposium (IEEE Cat. No. 02CH37313)*, 2002, vol. 2, pp. 392-395: IEEE.
- [16] H. Jeong, M. M. Tentzeris, and S. Lim, "Frequency-Tunable Electromagnetic Absorber by Mechanically Controlling Substrate Thickness," *International Journal of Antennas and Propagation*, vol. 2018, 2018.
- [17] S. C. Bakshi and D. Mitra, "A FSS-Based Polarization Insensitive Switchable Rasorber/Absorber," in *2020 International Symposium on Electromagnetic Compatibility-EMC EUROPE*, 2020, pp. 1-4: IEEE.
- [18] U. Jamwal, N. Narang, D. Singh, and K. Yadav, "Development of an Analytical Approach to Design FSS Absorber as per User Requirement," *Transactions of the Indian National Academy of Engineering*, vol. 5, no. 4, pp. 739-748, 2020.
- [19] T. Liu and S.-S. Kim, "Design of Ultrawide Bandwidth Electromagnetic Wave Absorbers with Square Patch Frequency Selective Surfaces with Different Geometries," *Korean Journal of Metals and Materials*, vol. 58, no. 5, pp. 326-333, 2020.
- [20] X. Lv, S. J. Chen, A. Galehdar, W. Withayachumnankul, and C. Fumeaux, "Fast Semi-Analytical Design for Single-FSS-Layer Circuit-Analog Absorbers," *IEEE Open Journal of Antennas and Propagation*, vol. 1, pp. 483-492, 2020.
- [21] C. Sabah, O. Turkmen-Kucuksari, and G. Turhan-Sayan, "Metamaterial absorber-based sensor embedded into X-band waveguide," *Electronics letters*, vol. 50, no. 15, pp. 1074-1076, 2014.
- [22] O. T. Gunduz and C. Sabah, "Alternative design of left-handed metamaterial based on circular resonator and wire strip for waveguide configurations with sensing and absorber applications," *Optical Engineering*, vol. 54, no. 8, p. 087101, 2015.
- [23] O. T. Gunduz and C. Sabah, "A novel left-handed metamaterial based on circular resonator and wire strip for waveguide applications," in *2014 16th International Conference on Transparent Optical Networks (ICTON)*, 2014, pp. 1-4: IEEE.
- [24] C. Sabah, M. M. Taygur, and E. Y. Zoral, "Investigation of microwave metamaterial based on H-shaped resonator in a waveguide configuration and its sensor and absorber applications," *Journal of Electromagnetic Waves and Applications*, vol. 29, no. 6, pp. 819-831, 2015.
- [25] C. Sabah, "Perfect metamaterial absorbers with polarization angle independency in X-band waveguide," *Modern Physics Letters B*, vol. 30, no. 11, p. 1650186, 2016.
- [26] C. Sabah, "Realization of polarization-angle-independent fishnet-based waveguide metamaterial comprised of octagon shaped resonators with sensor and absorber applications," *Journal of Materials Science: Materials in Electronics*, vol. 27, no. 5, pp. 4777-4787, 2016.
- [27] C. Sabah and H. Roskos, "Numerical and experimental investigation of fishnet-based metamaterial in a X-band waveguide," *Journal of Physics D: Applied Physics*, vol. 44, no. 25, p. 255101, 2011.
- [28] H. Jeong, T. T. Nguyen, and S. Lim, "Subwavelength metamaterial unit cell for low-frequency electromagnetic absorber applications," *Scientific reports*, vol. 8, no. 1, pp. 1-7, 2018.
- [29] C. A. Balanis, *Antenna theory: analysis and design*. John Wiley & sons, 2016.
- [30] N. I. Landy, S. Sajuyigbe, J. J. Mock, D. R. Smith, and W. J. Padilla, "Perfect metamaterial absorber," *Physical review letters*, vol. 100, no. 20, p. 207402, 2008.